

ARTICLE



Chronic prostatitis/chronic pelvic pain syndrome impairs erectile function by inducing apoptosis in a rat model of experimental autoimmune prostatitis

Qi Gu^{1,2}, Jiaochen Luan^{1,2}, Mengchi Yu^{1,2}, Jiadong Xia¹✉ and Zengjun Wang¹✉

© The Author(s), under exclusive licence to Springer Nature Limited 2024

Over the years, numerous epidemiological studies have shown that chronic prostatitis/chronic pelvic pain syndrome (CP/CPPS) promotes erectile dysfunction. Nonetheless, the precise underlying mechanism remains to be fully clarified. The objective of this research was to identify crucial signaling pathways responsible for CP/CPPS-induced erectile dysfunction. Thirty 8-week-old male Sprague–Dawley rats were randomly assigned to either the CP/CPPS model group or the control group. The CP/CPPS rat model was established through subcutaneous injection of a combination of rat prostate protein and Freund's adjuvant. Penile erectile function assessment was conducted 45 days after immunization through electrical stimulation of the cavernous nerve. RNA sequencing of the corpus cavernosum of the penis was then performed using the Kyoto Encyclopedia of Genes and Genomes and protein–protein interaction network analysis. Western blotting was performed on the cavernous tissue. Cell apoptosis assays, cell counting kit-8 assays, cell cloning assays, and Western blotting were conducted on rat endothelial cells. Erectile function was significantly lower in the CP/CPPS model group than in the control group ($p < 0.001$). Kyoto Encyclopedia of Genes and Genomes pathway analysis revealed that differentially expressed genes were predominantly enriched in the apoptosis pathway. Moreover, an increase in apoptosis in the rat corpus cavernosum, along with a decrease in the protein expression of CD31 ($p = 0.0089$) and eNOS ($p = 0.0069$) following CP/CPPS induction, was observed. In a protein–protein interaction network, Pitx2 was recognized as a central gene. The role of Pitx2 in regulating apoptosis was demonstrated in experiments using rat endothelial cell lines, and it was found to be regulated by the Wnt/ β -catenin pathway. This study highlights the occurrence of cavernous endothelial cell apoptosis in CP/CPPS-induced erectile dysfunction, and the potential mechanism of apoptosis may involve inhibition of the Wnt/ β -catenin/Pitx2 pathway.

IJIR: Your Sexual Medicine Journal; <https://doi.org/10.1038/s41443-024-00965-9>

INTRODUCTION

As a prevalent urinary system disorder, chronic prostatitis/chronic pelvic pain syndrome (CP/CPPS) affects adult males of various age groups, particularly those under the age of 50 [1–3]. An increasing body of research suggests a clear and positive association between erectile dysfunction (ED) and CP/CPPS. Studies estimate that the occurrence of ED among men with CP/CPPS varies from 15.0% to 61.5% [4–8]. The risk of developing ED is 3.62 times greater for those with CP/CPPS than for those without CP/CPPS, and it appears that ED severity correlates with prostatitis-like symptoms [5, 6]. Due to the high prevalence of patients diagnosed with CP/CPPS [1], a significant proportion of individuals who present with ED are diagnosed with this condition. Although phosphodiesterase type 5 inhibitors are commonly prescribed as the initial treatment for ED, a substantial subset of patients with CP/CPPS do not experience improvement in erectile function following this therapy [9]. Therefore, investigating the specific mechanisms through which CP/CPPS contributes to ED is essential for identifying novel and efficacious therapeutic interventions.

Transcriptome sequencing, a high-throughput technique, is commonly employed in the investigation of diverse diseases, enabling comprehensive analysis of gene expression profiles to elucidate disease-related molecular mechanisms and biological pathways [10–12]. This approach has been applied to investigate the pathogenesis of several forms of ED, such as diabetes mellitus-induced ED [13], cavernous nerve injury ED [14], and age-associated ED [15]. However, RNA sequencing has not yet been utilized in studies of CP/CPPS-induced ED to explore its pathogenesis.

It is now understood that in response to sexual stimulation, parasympathetic nervous system activity occurs, and endothelial nitric oxide synthase (eNOS) generates nitric oxide (NO), which diffuses into adjacent smooth muscle cells. Subsequently, NO activates guanylate cyclase, elevating cyclic guanosine monophosphate levels. This process increases the intracellular calcium concentration. As a consequence, smooth muscles relax, and blood flow increases [16–18]. Shoskes et al. [19] reported elevated levels of endothelial dysfunction and arterial stiffness in males suffering from CP/CPPS. Additionally, a recent investigation revealed a key

¹Department of Urology, The First Affiliated Hospital of Nanjing Medical University, No. 300 Guangzhou Road, Nanjing 210029, China. ²These authors contributed equally: Qi Gu, Jiaochen Luan, Mengchi Yu. ✉email: dongjiaxianjmu@sina.com; zengjunwang@njmu.edu.cn

Received: 8 February 2024 Revised: 3 August 2024 Accepted: 13 August 2024

Published online: 21 August 2024

genetic link between ED and CP/CPPS, which was predominantly enriched in corpus cavernosum endothelial cells [20]. While prior research has indicated that CP/CPPS can lead to impairment of corpus cavernosum endothelial cells [21], the specific signaling pathway responsible for this effect remains unknown.

Experimental autoimmune prostatitis (EAP) is commonly induced in rats by injecting prostate-specific antigens into rats, resulting in the immune system attacking its own prostate tissue [22]. This model closely mimics the symptoms, pathology, and immunological characteristics of human CP/CPPS, making it a valuable tool for investigating CP/CPPS-related conditions, including CP/CPPS-induced ED [23, 24]. In this study, an EAP rat model was established, and RNA sequencing of the corpus cavernosum was conducted to elucidate the mechanisms involved in CP/CPPS-induced ED and identify potential therapeutic targets.

MATERIALS AND METHODS

Animal procedures

In total, forty 8-week-old male Sprague–Dawley rats were obtained from the Experimental Animal Center of Nanjing Medical University. The weight of the rats ranged from 230 to 250 grams. The animals were housed at 25 °C with a 12-h light-dark cycle (lights on from 8:00 to 20:00). The Animal Ethics Committee of Nanjing Medical University provided ethical approval (No. IACUC-2307055).

Ten rats were humanely euthanized for the preparation of cell suspensions from homogenized prostate tissues. A random assignment was conducted using the random number table method for the remaining thirty rats, either the EAP group or the control group ($n = 15$ rats per group). The EAP model protocol has already been described in detail [23]. Briefly, EAP rats received multiple subcutaneous injections of a 1.0 mL isovolumetric mixture containing 20 mg/mL prostate tissue supernatant and Freud's complete adjuvant (Sigma Aldrich, Saint-Louis, Missouri, USA). A similar volume of phosphate-buffered saline (PBS) was injected into the control group rats. Autoimmune injections were administered on Days 0, 15, and 30.

Erectile function evaluation

Assessment of erectile function took place 45 days postimmunization. The evaluation involved measuring the highest intracavernous pressure (ICP) and calculating the ratio between the maximum ICP and the mean arterial pressure (MAP), as previously described [23]. The electrical stimulation parameters were set as 5 V, 15 Hz, and 0.2 ms width. Each stimulation lasted for 1 min with a 5-min interval. Pressure measurements and electrical stimulation were carried out using a BL-420S Biological Functional System (Chengdu Taimeng Technology Co., Ltd., Chengdu, Sichuan, China). Each experiment was conducted in triplicate. All tests were administered by a single operator who was blind to the groupings.

RNA sequencing

Total RNA was extracted from rat penile cavernous tissues with TRIzol reagent (Invitrogen, Waltham, MA, USA). RNA quality was evaluated using a NanoDrop spectrophotometer (Thermo Fisher Scientific, Waltham, Massachusetts, USA). Then, samples were prepared using three micrograms of RNA. Sequencing libraries were generated in several steps. Initially, poly-T oligo-attached magnetic beads were utilized to extract mRNA from total RNA. To achieve fragmentation, divalent cations in fragmentation buffer (Illumina, San Diego, CA, USA) were used, followed by the synthesis of cDNA. Amplification with the AMPure XP system (Beckman Coulter, Beverly, CA, USA) was used to select cDNA fragments that were 400–500 bp in length. After 15 cycles of PCR with an Illumina PCR Primer Cocktail, DNA fragments with ligated adaptor molecules at both ends were selectively enriched. The purified products were quantified using Agilent's high-sensitivity DNA analyzer (Agilent, Santa Clara, CA, USA). The adaptors and low-quality bases were trimmed using Cutadapt v1.15 software (<https://github.com/marcelm/cutadapt/>). Gene annotation and reference genome files were downloaded, and the filtered reads were mapped using HISAT2 v2.0.5 (<http://daehwankimlab.github.io/hisat2/>).

Bioinformatics analysis

Differentially expressed genes (DEGs) were identified using the R Bioconductor program DESeq2, with a cutoff of $p < 0.05$.

To explore the functional enrichment of different genes, Gene Ontology and Kyoto Encyclopedia of Genes and Genomes (KEGG) analyses (<https://www.genome.jp/kegg>) were conducted with the Bioconductor package clusterProfiler.

The Search Tool for Retrieval of Interacting Genes (STRING, <http://www.string-db.org>) was used to generate a protein–protein interaction (PPI) network. The minimum interaction score was set at 0.15, and protein nodes with no interactions were excluded. CytoHubba (degree ranking method) was then used to calculate and visualize the top 5 genes with Cytoscape V3.8.2 software (<https://cytoscape.org/>).

Histopathology

Following euthanasia with pentobarbital sodium (40 mg/kg), prostate and penis tissues were harvested and rinsed with PBS. Sections of prostate and penis tissues were fixed for 24 hours in 4% paraformaldehyde and cut into 5 μ m thick sections. The remaining tissues were stored at -80 °C for subsequent experiments. Hematoxylin and eosin staining was performed on the prostate tissue sections, while apoptosis in the corpus cavernosum was detected using the TUNEL assay following the TUNEL Apoptosis Assay Kit protocol (Vazyme, Nanjing, Jiangsu, China). A Zeiss LSM5 live confocal microscope was used to capture immunofluorescence images (Carl Zeiss Meditec, Oberkochen, Germany).

Measurement of serum TNF- α and IL-1 β levels

Serum was obtained by collecting and centrifuging blood samples from the inferior vena cava at 4 °C following an assessment of erectile function. An enzyme-linked immunosorbent assay kit (Gelatin, Shanghai, China) was used to evaluate the levels of TNF- α and IL-1 β following the manufacturer's instructions.

RNA extraction and quantitative real-time PCR (qRT–PCR)

Total RNA was extracted, and cDNA was generated using HiScript II reagent (Vazyme, Nanjing, Jiangsu, China). A SYBR premix kit from Vazyme was used to determine mRNA levels through qRT–PCR on a LightCycler 480 from Roche, USA. The sequences of primers used for TsingKe (Nanjing, Jiangsu, China) are listed in Table S1.

Protein extraction and Western blotting

Using RIPA buffer (Beyotime, Shanghai, China), proteins were extracted from tissues and cells. Subsequently, the separated protein samples were transferred onto polyvinylidene fluoride membranes (Millipore, Bedford, MA, USA) by SDS–PAGE. After the blocking step (G7205, GBCBIO, Guangzhou, China), the membranes were incubated overnight at 4 °C with primary antibodies specific for Bax (1:1 000, Abmart, Shanghai, China), Bcl-2 (1:1 000, Abmart, Shanghai, China), cleaved caspase-3 (1:1 000, OriGene, Rockville, Maryland, USA), CD 31 (1:5 000, Proteintech, Wuhan, Hubei, China), eNOS (1:2 000, Abmart, Shanghai, China), Pitx2 (1:1 000, Santa Cruz Biotechnology, Santa Cruz, CA, USA), c-Myc (1:5 000, Proteintech, Wuhan, Hubei, China), Cyclin D1 (1:1 000, Cell Signaling Technology, Danvers, MA, USA), β -catenin (1:2 000, Abcam, Cambridge, MA, USA), GSK3 β (1:1 000, Cell Signaling Technology, Danvers, MA, USA), p-GSK3 β (1:1 000, Abmart, Shanghai, China), β -Tubulin (1:5 000, Proteintech, Wuhan, Hubei, China) and GAPDH (1:1,000, Cell Signaling Technology), followed by the appropriate secondary antibodies (1:10 000, Cell Signaling Technology, Danvers, MA, USA). Protein visualization was achieved using chemiluminescence (Bio-Rad, Hercules, CA, USA).

Cell culture

Procell Life Science & Technology Co., Ltd. (Wuhan, Hubei, China) supplied the rat aortic endothelial cells (RAOECs) for this study. The cells were cultured in high-glucose DMEM (C3113-0500, Vivacell, Shanghai, China) supplemented with 10% FBS (16000044, Gibco, Grand Island, NY, USA) at 37 °C in 5% CO₂. MSAB (HY-120697, MedchemExpress, Monmouth Junction, NJ, USA) was dissolved in DMSO to achieve a final DMSO concentration of less than 0.1%, serving as an inhibitor of the Wnt/ β -catenin signaling pathway.

Transfection of siRNAs

GeneRay Biotechnology (Shanghai, China) designed and synthesized rat Pitx2-specific siRNAs (siRNA-Pitx2) and the negative control. The transfection process was carried out according to the manufacturer's instructions using Lipofectamine 3000 reagent (L3000015, Invitrogen, Waltham, MA,

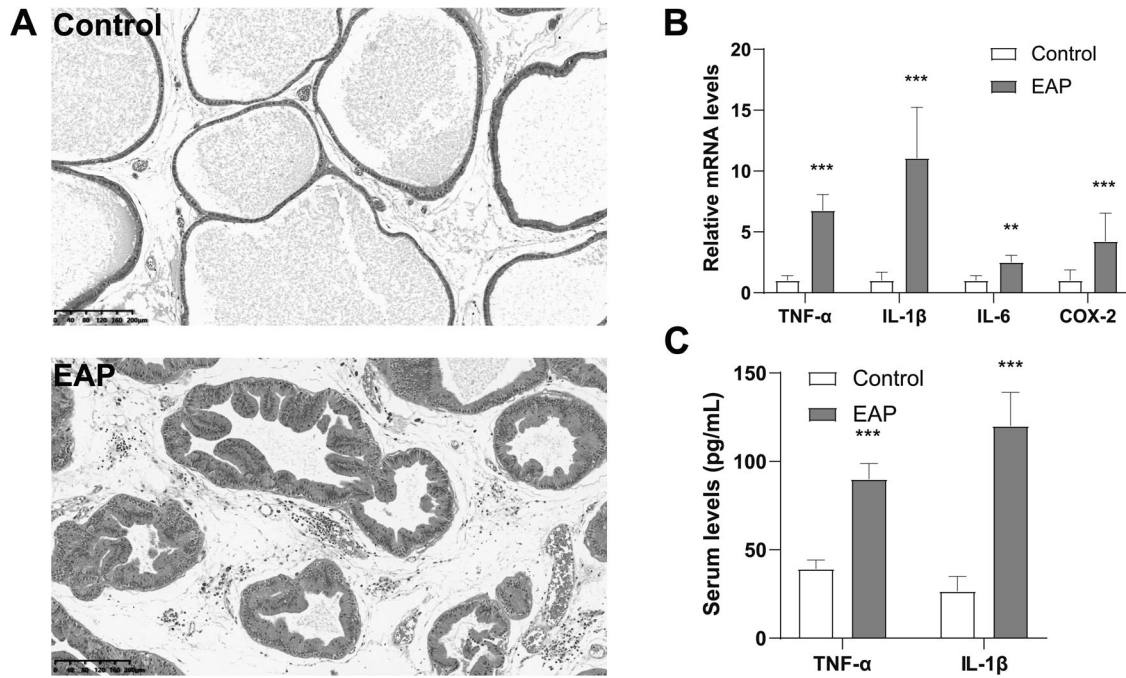


Fig. 1 Establishment of the experimental autoimmune prostatitis rat model. **A** Representative images of hematoxylin and eosin staining of the rat prostate (scale bars = 200 μ m). **B** Relative mRNA levels of TNF- α , IL-1 β , IL-6, and COX-2 compared with those of GAPDH. **C** Serum levels of TNF- α and IL-1 β . The data are presented as the means \pm standard deviations ($n = 6$). ** $p < 0.01$, *** $p < 0.001$ indicate a significant difference between the two groups.

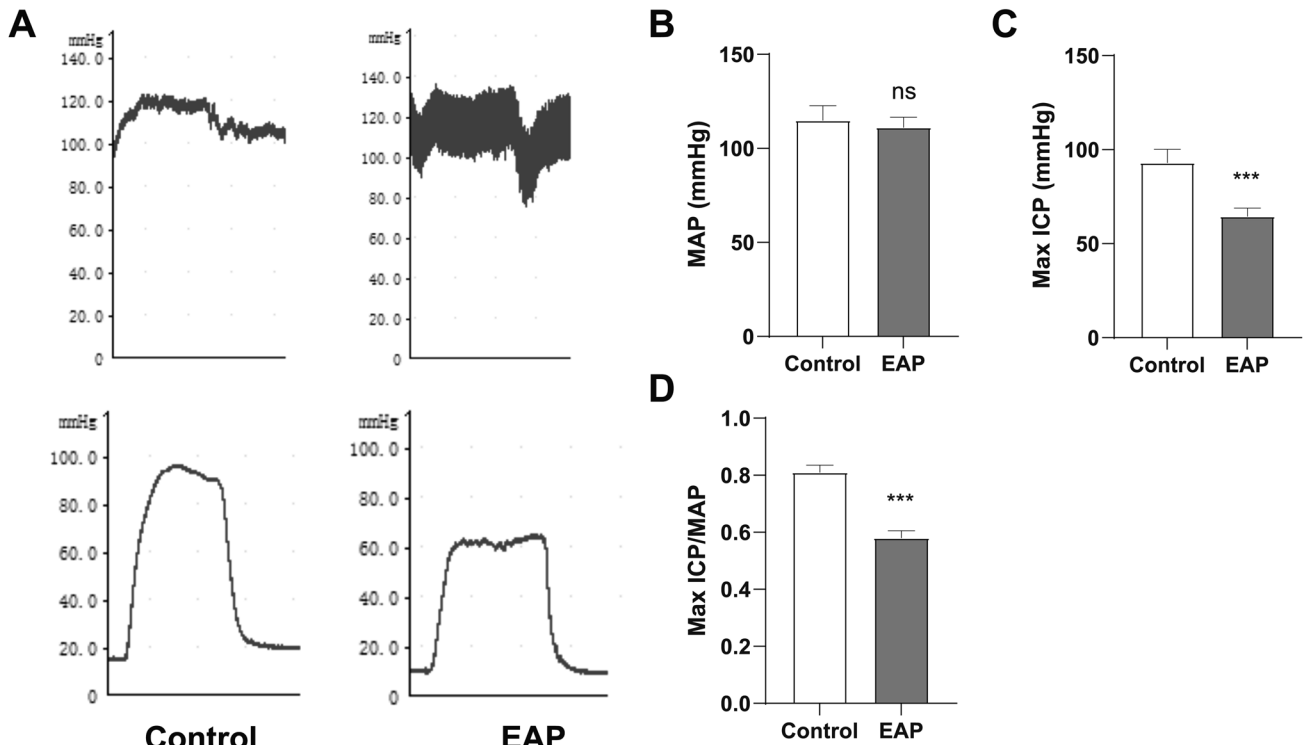


Fig. 2 Assessment of erectile function. **A** Representative recordings of mean arterial pressure (MAP) and intracavernous pressure (ICP) during 1 min of electrical stimulation at 5.0 V and 15 Hz. **B** Statistical analysis of the MAP levels. **C** Statistical analysis of the maximum ICP. **D** Erectile function according to the maximum ICP/MAP ratio. The data are presented as the means \pm standard deviations ($n = 8$). *** $p < 0.001$ indicates a significant difference between the two groups.

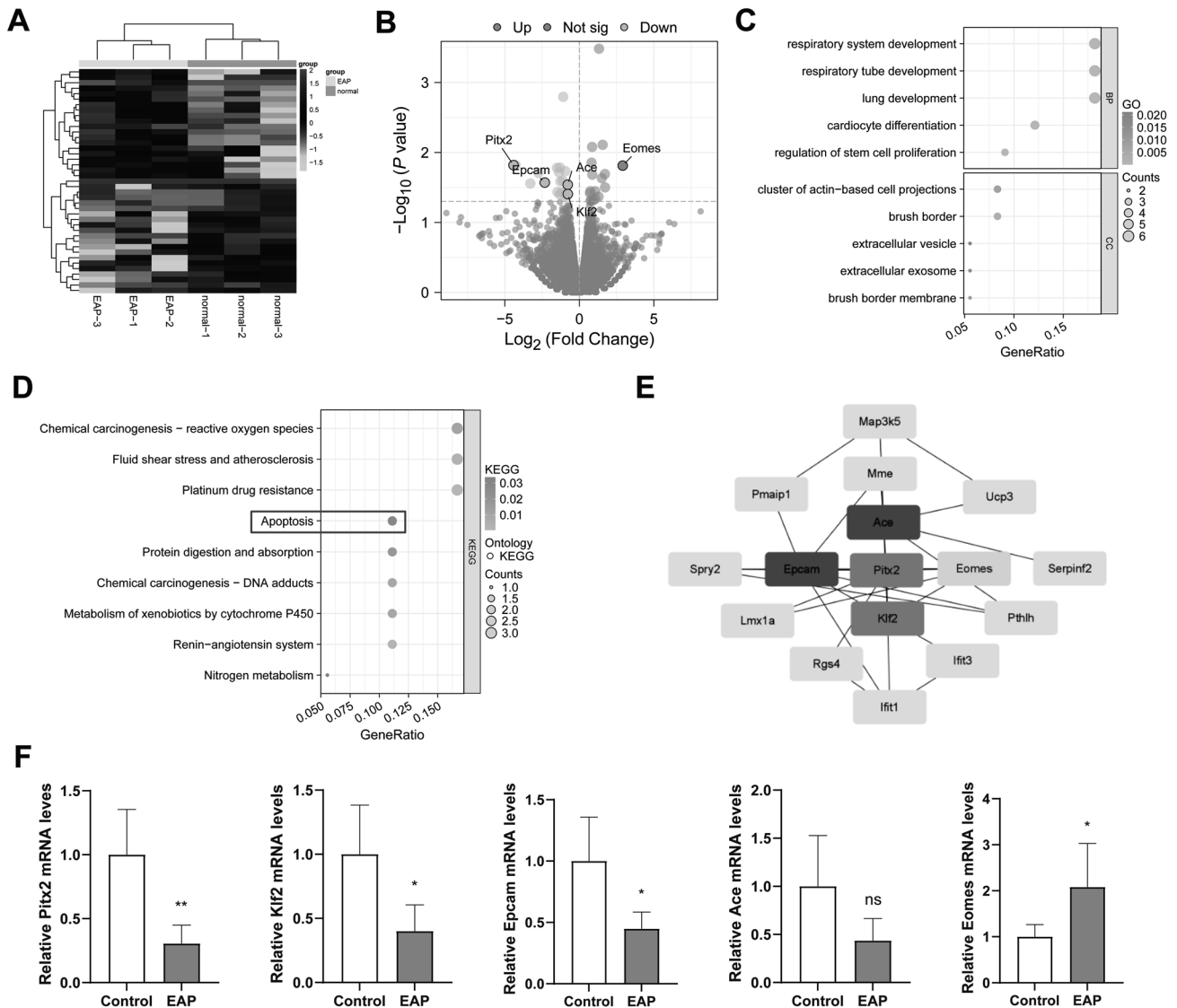


Fig. 3 Transcriptome analysis of rat corpus cavernosum. **A** Heatmap showing the differentially expressed genes (DEGs). **B** Volcano plots showing the DEGs. **C** Gene Ontology enrichment of the DEGs. **D** Kyoto Encyclopedia of Genes and Genomes pathway of the DEGs with the apoptosis pathway highlighted. **E** Protein-protein interaction network analysis and hub gene interaction analysis using Cytoscape software. **F** Verification of hub gene expression by qRT-PCR. The data are presented as the means \pm standard deviations ($n = 5$). * $p < 0.05$, ** $p < 0.01$ indicate a significant difference between the two groups.

USA). Subsequent experiments were conducted 48 hours after transfection. Table S2 displays the sequences of siRNA-Pitx2.

Cell apoptosis assay

Using an Annexin V-FITC/PI Apoptosis Detection Kit, the harvested RAOECs were stained with FITC-labeled Annexin V and propidium iodide for 10 minutes (Vazyme, Nanjing, Jiangsu, China). Flow cytometry was then performed on the stained cells using a CytoFLEX (Beckman Coulter, Beverly, CA, USA).

Cell proliferation assay

A cell counting kit-8 (CCK-8, Vazyme, Nanjing, Jiangsu, China) was used to determine the proliferation rate of 500 cells plated in 96-well plates. During one hour of incubation, the medium containing 10% CCK-8 was replaced with the original medium. A microplate reader (Tecan, Mannedorf, Switzerland) was used to measure the absorbance at 450 nm.

Colony formation assay

In 6-well plates, 500 cells were seeded. The fixative 4% paraformaldehyde was applied after 7 days, and crystal violet was added. ImageJ software

(National Institutes of Health, Bethesda, MD, USA) was used to visualize and quantify the cell colonies.

Statistical analysis

The statistical analysis was conducted utilizing IBM SPSS 22.0 (Armonk, NY, USA). To compare discrepancies, Student's *t* tests were employed, where statistical significance was determined by a two-sided *p* value less than 0.05.

RESULTS

Establishment of an EAP rat model

Compared with those in the control group, the prostate glands in the EAP group exhibited partial atrophy of the glandular epithelium structure. The acinar epithelium appeared flattened, and the stroma displayed significant infiltration of inflammatory cells, along with small vessel hyperplasia (Fig. 1A). qRT-PCR analysis of prostate tissues revealed elevated levels of the inflammatory cytokines TNF- α , IL-1 β , COX-2 and IL-6 in EAP model rats ($p < 0.001$, $p < 0.001$, $p < 0.001$ and $p = 0.0093$, respectively;

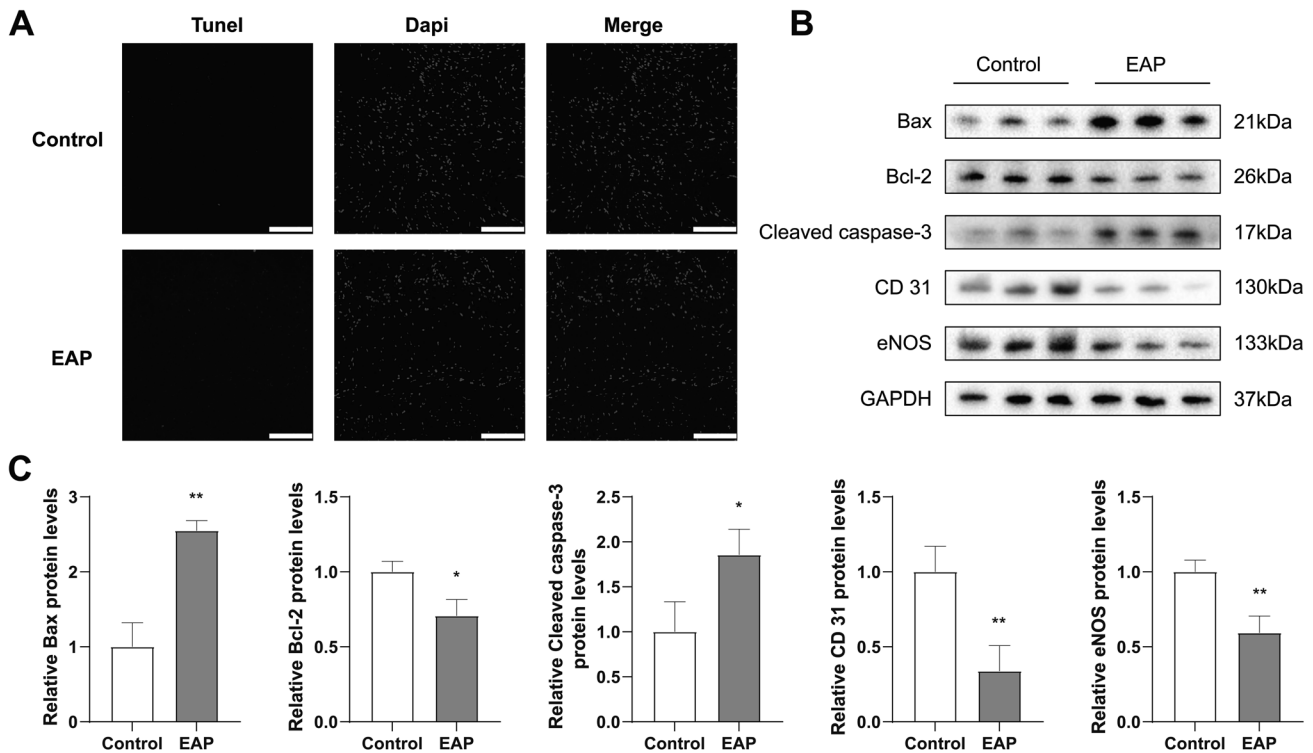


Fig. 4 The expression levels of genes related to apoptosis and endothelial cells. **A** Representative immunofluorescence results showing apoptosis in the corpus cavernosum by TUNEL assay (scale bars = 100 μ m). **B** Representative WB bands showing Bax, Bcl-2, cleaved caspase-3, CD31 and eNOS expression. **C** Statistical analysis of the WB results. The data are presented as the means \pm standard deviations ($n = 3$). * $p < 0.05$, ** $p < 0.01$ indicate a significant difference between the two groups.

Fig. 1B). Compared with those in the control group, the serum levels of TNF- α ($p < 0.001$) and IL-1 β ($p < 0.001$) in the EAP group were notably elevated (Fig. 1C).

Erectile function

Figure 2 shows that the EAP rats had a considerably lower maximum ICP/MAP ratio ($p < 0.001$) than did the control rats, indicating the successful induction of erectile dysfunction through EAP.

Transcriptome analysis of the rat corpus cavernosum

There were 41 differentially expressed genes (DEGs) identified, with 21 downregulated and 20 upregulated DEGs (Fig. 3A, B). Gene Ontology enrichment results revealed the following enriched terms for the DEGs in the biological process (BP) category: respiratory system development, respiratory tube development and lung development, cardiomyocyte differentiation and regulation of stem cell proliferation. The following DEGs were enriched in the cellular component (CC) category: cluster of actin-based cell projections, brush border, extracellular vesicle, extracellular exosome and brush border membrane (Fig. 3C). KEGG analysis revealed significant enrichment of DEGs related to chemical carcinogenesis-reactive oxygen species, fluid shear stress and atherosclerosis, platinum drug resistance and apoptosis (Fig. 3D). The PPI network was then analyzed, and cytoHubba was utilized to calculate and identify the top five genes (*Ace*, *Epcam*, *Pitx2*, *Eomes*, and *Klf2*) via Cytoscape software (Fig. 3E). qRT-PCR confirmed the identity of the hub genes, with *Pitx2* exhibiting the most significant difference (*Ace*: $p = 0.0599$; *Epcam*: $p = 0.0123$; *Pitx2*: $p = 0.0037$; *Eomes*: $p = 0.0395$; *Klf2*: $p = 0.0150$; Fig. 3F).

Expression of apoptosis marker, CD31, and eNOS in the corpus cavernosum

A greater level of apoptosis was observed in the EAP group (Fig. 4A). The levels of Bax ($p = 0.0015$) and cleaved caspase-3

($p = 0.0280$) were also significantly increased. In addition, there was a notable decrease in the expression of CD31 ($p = 0.0089$) and eNOS ($p = 0.0069$) in EAP rats (Fig. 4B, C).

Knockdown of Pitx2 impaired the function of RAOEC

Western blotting (Fig. 5A) confirmed the effectiveness of Pitx2 knockdown. In response to the downregulation of Pitx2, RAOEC proliferation was reduced (Fig. 5B, C), while the apoptosis rate was significantly increased (Fig. 5D). As determined by Western blotting, si-Pitx2 cells showed significant reductions in c-Myc, Cyclin D1 and Bcl-2 levels (si1 vs. siCtrl: $p = 0.0107$, $p = 0.0147$ and $p = 0.0279$, respectively; si2 vs. siCtrl: $p = 0.0315$, $p = 0.0234$ and $p = 0.0262$, respectively), accompanied by an increase in Bax and cleaved caspase-3 levels (si1 vs. siCtrl: $p = 0.0143$ and $p = 0.0166$, respectively; si2 vs. siCtrl: $p = 0.0148$ and $p = 0.0026$, respectively; Fig. 5E, F).

The Wnt/ β -catenin signaling pathway regulated Pitx2 in the corpus cavernosum

Previous studies have reported that Pitx2 is a downstream target of the Wnt/ β -catenin signaling pathway, and this association was validated in RAOECs using MSAB (10 μ M). After 12 hours of MSAB treatment, the protein level of Pitx2 was decreased ($p = 0.0192$), which was consistent with the reduced expression of β -catenin and p-GSK3 β ($p = 0.0248$ and $p = 0.0294$, respectively, Fig. 6A, B). Moreover, a similar effect was detected in the rat corpus cavernosum (β -catenin, $p = 0.0326$; p-GSK3 β , $p = 0.0054$; pitx2, $p = 0.0052$; Fig. 6C, D).

DISCUSSION

ED is a prevalent male complication of CP/CPPS that significantly impacts the well-being and quality of life of afflicted individuals [5, 25]. Current treatment modalities have demonstrated limited

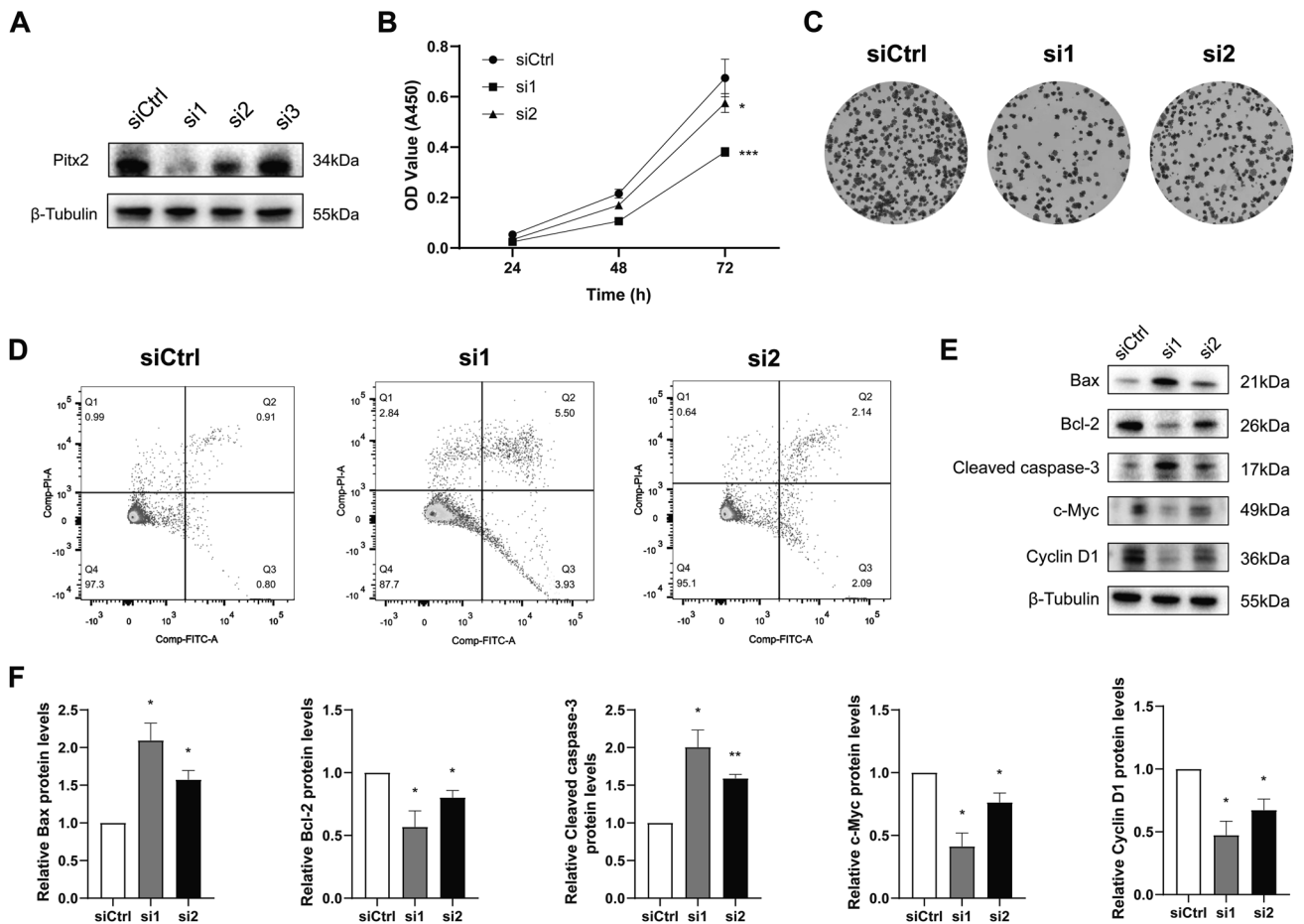


Fig. 5 Knockdown of Pitx2 promoted apoptosis and suppressed proliferation of rat aortic endothelial cells (RAOECs). **A** The verification of siRNA-Pitx2 efficiency by WB. **B** Cell Counting Kit-8 assay. **C** Colony formation assay. **D** Cell apoptosis detection by flow cytometry. **E** Representative WB bands showing Bax, Bcl-2, cleaved caspase-3, c-Myc and Cyclin D1 expression. **F** Statistical analysis of the WB results. The data are presented as the means \pm standard deviations ($n = 3$). * $p < 0.05$, ** $p < 0.01$ indicate a significant difference between the siCtrl group and the si1 (si2) group.

efficacy in managing this dysfunction [9]. Investigating the pathogenesis of CP/CPPS-induced ED, with a specific focus on genetic targets within the corpus cavernosum, may present a promising therapeutic approach for this condition. In this study, we established an EAP rat model to simulate human CP/CPPS, and decreased erectile function was observed in EAP model rats. The findings of the experiment indicated an increase in apoptosis and a decrease in endothelial cell number within rat cavernous tissues. Pitx2 was identified as a crucial gene in ED induced by CP/CPPS, and its expression was modulated by the Wnt/ β -catenin pathway. The impact of Pitx2 on the apoptosis and proliferation of rat endothelial cells was validated in vitro, while inhibition of the Wnt/ β -catenin pathway was observed in cavernous tissue from the EAP group.

Apoptosis, a regulated cellular death process governed by intrinsic programming, serves as a critical mechanism in biological functions [26]. Studies have indicated that apoptosis largely contributes to the pathogenesis of ED resulting from diverse etiological factors, such as diabetes [27], nerve injury [28], and advanced age [29]. Furthermore, CP/CPPS has been shown to induce apoptosis in the corpus cavernosum of rats [23]. In our investigation, KEGG analysis indicated the involvement of the apoptosis pathway in ED induced by CP/CPPS. Immunofluorescence assays revealed an increased level of apoptosis in the cavernous tissue of EAP model rats. Furthermore, Western blotting demonstrated an elevated Bax/Bcl-2 ratio and cleaved caspase-3 level in the cavernous tissue of EAP model rats. Endothelial cells play a

crucial role in the production of NO by expressing eNOS to maintain erectile function [16, 17]. Hu et al. [23] demonstrated a reduction in eNOS levels in the cavernous tissue of rats with EAP, indicating potential damage to cavernous endothelial cells. Similarly, our study revealed a decrease in eNOS levels, as well as a reduction in the level of CD31, an endothelial marker, suggesting a decrease in the number of cavernous endothelial cells.

Pitx2, a gene belonging to the bicoid/paired-like homeobox family on chromosome 4q25, regulates left-right asymmetry and multiple organ development [30, 31]. Recent studies have emphasized the role of Pitx2 in promoting cell proliferation and preventing apoptosis in various tissues and cells. Several studies have implicated it in the development and progression of hepatocellular carcinoma, colorectal cancer, and many other tumors [32–34]. According to Acunzo et al. [35], inactivating Pitx2 causes tumor cells to undergo apoptosis. Our findings indicate that Pitx2 may play a key gene in CP/CPPS-induced ED, as suggested by the PPI network analysis. Reduced expression of Pitx2 was consistently observed in the cavernous tissue of rats in the EAP group and correlated with the level of apoptosis. In vitro experiments further demonstrated that knockdown of Pitx2 led to increased apoptosis in rat endothelial cells. This study represents the first documentation of the role of the Pitx2 gene in the development of CP/CPPS-induced ED.

Early literature has extensively reported the close relationship between Pitx2 and the Wnt/ β -catenin pathway [36–38]. Phosphorylated β -catenin, for example, enters the nucleus to activate

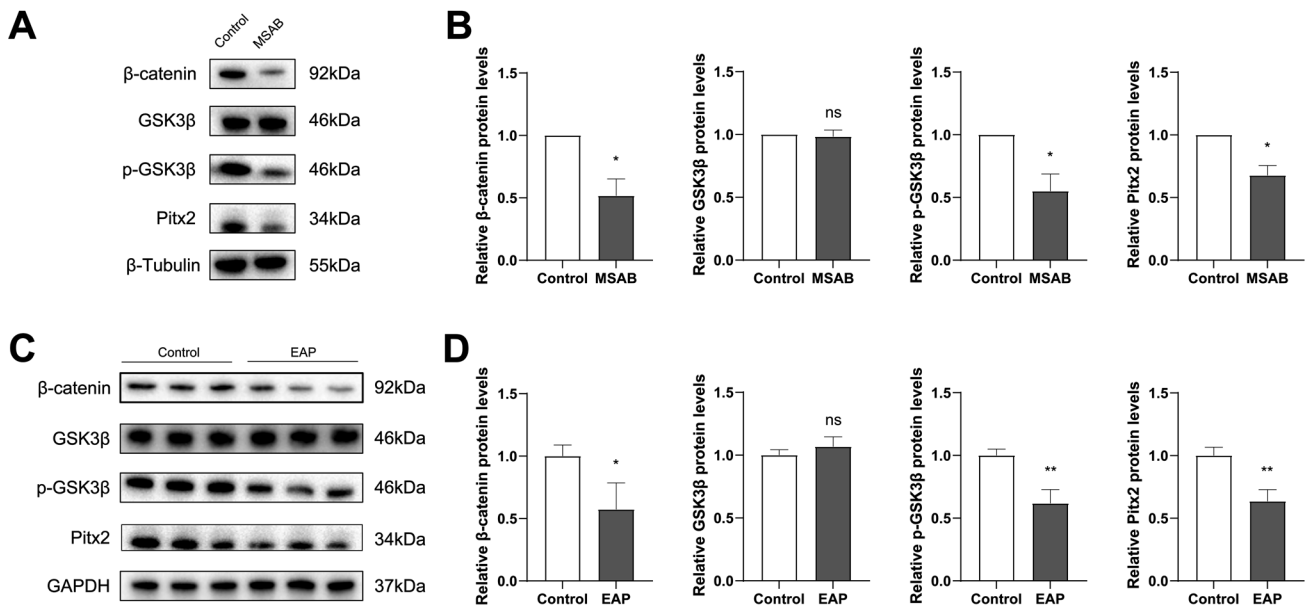


Fig. 6 Members of the Wnt/ β -catenin/Pitx2 signaling pathway were downregulated. **A** Representative WB bands of β -catenin, GSK3 β , p-GSK3 β and Pitx2 in RAOECs treated with an inhibitor of the Wnt/ β -catenin signaling pathway (MSAB, 10 μ M, 12 h). **B** Statistical analysis of the WB results. **C** Representative WB bands showing the levels of β -catenin, GSK3 β , p-GSK3 β and Pitx2 in the rat corpus cavernosum. **D** Statistical analysis of the WB results. The data are presented as the means \pm standard deviations ($n = 3$). * $p < 0.05$, ** $p < 0.01$ indicate a significant difference between the two groups.

the expression of downstream target genes, including Pitx2, which in turn targets the expression of cell cycle regulators such as Cyclin D1 and c-Myc [39]. Several other studies have reported the effect of Pitx2 on the activation of the Wnt/ β -catenin signaling pathway [33, 37]. Notably, the protective role of this pathway in the vascular endothelium has been established. For instance, Sun et al. reported that acidic fibroblast growth factor alleviates diabetic endothelial dysfunction by reducing oxidative stress through Wnt/ β -catenin-mediated upregulation of hexokinase 2 [40]. Another study revealed that β -catenin and GSK3 β were upregulated during angiogenesis and vascular repair in TNF- α -induced human brain microvascular endothelial cells [41]. Our research findings indicated that Pitx2 was regulated by the Wnt/ β -catenin pathway in rat endothelial cells, as demonstrated by in vitro experiments. Additionally, reductions in the levels of β -catenin and p-GSK3 β were observed in EAP model rat cavernous tissue, suggesting that targeting gene inhibitors in this pathway could be a promising therapeutic approach. However, it is important to acknowledge the limitations of our study. First, in vitro experiments were not conducted in the context of CP/CPSPS due to the absence of suitable models. Second, our investigation detected only the expression of Wnt/ β -catenin/Pitx2 pathway members in cavernous tissue and did not alter the activation of this pathway. Genetic intervention targeting this pathway directly in the penis will be the focus of our future research.

CONCLUSION

In conclusion, an increase in cavernous endothelial cell apoptosis was observed in CP/CPSPS-induced ED, and the suppression of the Wnt/ β -catenin/Pitx2 pathway potentially served as a key mechanism. These findings provide new insight into the pathogenesis of CP/CPSPS-induced ED and suggest potential therapeutic targets.

DATA AVAILABILITY

The data that support the findings of this study are available from the corresponding author upon reasonable request.

REFERENCES

- Schaeffer AJ, Landis JR, Knauss JS, Probert KJ, Alexander RB, Litwin MS, et al. Demographic and clinical characteristics of men with chronic prostatitis: the national institutes of health chronic prostatitis cohort study. *J Urol*. 2002;168:593–8.
- Rees J, Abrahams M, Doble A, Cooper A. Diagnosis and treatment of chronic bacterial prostatitis and chronic prostatitis/chronic pelvic pain syndrome: a consensus guideline. *BJU int*. 2015;116:509–25.
- Graziani A, Grande G, Martin M, Ferraioli G, Colonnello E, Iafraite M, et al. Chronic prostatitis/chronic pelvic pain syndrome and male infertility. *Life (Basel)*. 2023;13:1700.
- Bartoletti R, Cai T, Mondaini N, Dinelli N, Pinzi N, Pavone C, et al. Prevalence, incidence estimation, risk factors and characterization of chronic prostatitis/chronic pelvic pain syndrome in urological hospital outpatients in Italy: results of a multicenter case-control observational study. *J Urol*. 2007;178:2411–5.
- Chung SD, Keller JJ, Lin HC. A case-control study on the association between chronic prostatitis/chronic pelvic pain syndrome and erectile dysfunction. *BJU int*. 2012;110:726–30.
- Zhang Z, Li Z, Yu Q, Wu C, Lu Z, Zhu F, et al. The prevalence of and risk factors for prostatitis-like symptoms and its relation to erectile dysfunction in Chinese men. *Andrology*. 2015;3:1119–24.
- Lee SW, Liong ML, Yuen KH, Leong WS, Cheah PY, Khan NA, et al. Adverse impact of sexual dysfunction in chronic prostatitis/chronic pelvic pain syndrome. *Urology*. 2008;71:79–84.
- Hao ZY, Li HJ, Wang ZP, Xing JP, Hu WL, Zhang TF, et al. The prevalence of erectile dysfunction and its relation to chronic prostatitis in Chinese men. *J Androl*. 2011;32:496–501.
- Yan C, Huang Y, Wen D, Hou J, Pu J, Ouyang J, et al. The effect of sildenafil in the treatment of chronic non-bacteria prostatitis and concomitant erectile dysfunction. *Chin J Urol*. 2005;26:626–8.
- Zhang Y, Li Y, Zhou L, Yuan X, Wang Y, Deng Q, et al. Nav1.8 in keratinocytes contributes to ROS-mediated inflammation in inflammatory skin diseases. *Redox Biol*. 2022;55:102427.
- Xiong Y, Liu Y, Cao L, Wang D, Guo M, Jiang A, et al. Transcriptomic characteristics of bronchoalveolar lavage fluid and peripheral blood mononuclear cells in COVID-19 patients. *Emerg Microbes Infect*. 2020;9:761–70.
- Chen T, Yang S, Xu J, Lu W, Xie X. Transcriptome sequencing profiles of cervical cancer tissues and SiHa cells. *Funct Integr Genomics*. 2020;20:211–21.
- Kang JQ, Song YX, Liu L, Lu Y, Tian J, Hu R, et al. Identification of key genes in type 2 diabetes-induced erectile dysfunction rats with stem cell therapy through high-throughput sequencing and bioinformatic analysis. *Andrologia*. 2021;53:e14031.
- Kim MY, Jo MS, Choi SG, Moon HW, Park J, Lee JY. Repeated injections of mesenchymal stem cell-derived exosomes ameliorate erectile dysfunction in a

- cavernous nerve injury rat model. *World J Mens Health*. 2024; <https://doi.org/10.5534/wjmh.230218>.
15. Liu Q, Song Y, Cui Y, Hu C, Luo Y, Hu D, et al. Heterogeneity of fibroblasts is a hallmark of age-associated erectile dysfunction. *Int J Biochem Cell Biol*. 2023;156:106343.
 16. Burnett AL. Nitric oxide in the penis: physiology and pathology. *J Urol*. 1997; 157:320–4.
 17. Chitale K, Wingard CJ, Clinton Webb R, Branam H, Stopper VS, Lewis RW, et al. Antagonism of Rho-kinase stimulates rat penile erection via a nitric oxide-independent pathway. *Nat Med*. 2001;7:119–22.
 18. Hurt KJ, Sezen SF, Lagoda GF, Musicki B, Rameau GA, Snyder SH, et al. Cyclic AMP-dependent phosphorylation of neuronal nitric oxide synthase mediates penile erection. *Proc Natl Acad Sci USA*. 2012;109:16624–9.
 19. Shoskes DA, Prots D, Karns J, Horhn J, Shoskes AC. Greater endothelial dysfunction and arterial stiffness in men with chronic prostatitis/chronic pelvic pain syndrome—a possible link to cardiovascular disease. *J Urol*. 2011;186:907–10.
 20. Yuan P, Sun T, Han Z, Chen Y, Meng Q. Uncovering the genetic links of diabetic erectile dysfunction and chronic prostatitis/chronic pelvic pain syndrome. *Front Physiol*. 2023;14:1096677.
 21. Huang T, Wang G, Hu Y, Shi H, Wang K, Yin L, et al. Structural and functional abnormalities of penile cavernous endothelial cells result in erectile dysfunction at experimental autoimmune prostatitis rat. *J Inflamm (Lond)*. 2019;16:20.
 22. Kurita M, Yamaguchi H, Okamoto K, Kotera T, Oka M. Chronic pelvic pain and prostate inflammation in rat experimental autoimmune prostatitis: Effect of a single treatment with phosphodiesterase 5 inhibitors on chronic pelvic pain. *Prostate*. 2018;78:1157–65.
 23. Hu Y, Niu X, Wang G, Huang J, Liu M, Peng B. Chronic prostatitis/chronic pelvic pain syndrome impairs erectile function through increased endothelial dysfunction, oxidative stress, apoptosis, and corporal fibrosis in a rat model. *Andrology*. 2016;4:1209–16.
 24. Penna G, Fibbi B, Maggi M, Adorini L. Prostate autoimmunity: from experimental models to clinical counterparts. *Expert Rev Clin Immunol*. 2009;5:577–86.
 25. Zhang Y, Zheng T, Tu X, Chen X, Wang Z, Chen S, et al. Erectile dysfunction in chronic prostatitis/chronic pelvic pain syndrome: outcomes from a multi-center study and risk factor analysis in a single center. *PLoS one*. 2016;11:e0153054.
 26. Thompson CB. Apoptosis in the pathogenesis and treatment of disease. *Science*. 1995;267:1456–62.
 27. Liu K, Sun T, Luan Y, Chen Y, Song J, Ling L, et al. Berberine ameliorates erectile dysfunction in rats with streptozotocin-induced diabetes mellitus through the attenuation of apoptosis by inhibiting the SPHK1/S1P/S1PR2 and MAPK pathways. *Andrology*. 2022;10:404–18.
 28. Liu K, Sun T, Xu W, Song J, Chen Y, Ruan Y, et al. Relaxin-2 prevents erectile dysfunction by cavernous nerve, endothelial and histopathological protection effects in rats with bilateral cavernous nerve injury. *World J Mens Health*. 2023;41:434–45.
 29. Li K, Li R, Zhao Z, Feng C, Liu S, Fu Q. Therapeutic potential of mesenchymal stem cell-derived exosomal miR-296-5p and miR-337-3p in age-related erectile dysfunction via regulating PTEN/PI3K/AKT pathway. *Biomed Pharmacother*. 2023;167:115449.
 30. Logan M, Pagán-Westphal SM, Smith DM, Paganessi L, Tabin CJ. The transcription factor Pitx2 mediates situs-specific morphogenesis in response to left-right asymmetric signals. *Cell*. 1998;94:307–17.
 31. Campione M, Steinbeisser H, Schweickert A, Deissler K, van Bebber F, Lowe LA, et al. The homeobox gene Pitx2: mediator of asymmetric left-right signaling in vertebrate heart and gut looping. *Development*. 1999;126:1225–34.
 32. Xu YY, Yu HR, Sun JY, Zhao Z, Li S, Zhang XF, et al. Upregulation of PITX2 promotes letrozole resistance via transcriptional activation of IFITM1 signaling in breast cancer cells. *Cancer Res Treat*. 2019;51:576–92.
 33. Jiang L, Wang X, Ma F, Wang X, Shi M, Yan Q, et al. PITX2C increases the stemness features of hepatocellular carcinoma cells by up-regulating key developmental factors in liver progenitor. *J Exp Clin Cancer Res*. 2022;41:211.
 34. Shu Y, He C, Xiong Y, Lan J, Song R. Paired-like homeodomain transcription factor 2 strengthens chemoresistance in colorectal cancer by activating the Wnt/ β -catenin axis. *Neoplasma*. 2021;68:557–66.
 35. Acunzo J, Roche C, Defilles C, Thirion S, Quentien MH, Figarella-Branger D, et al. Inactivation of PITX2 transcription factor induced apoptosis of gonadotroph tumoral cells. *Endocrinology*. 2011;152:3884–92.
 36. Briata P, Ilengo C, Corte G, Moroni C, Rosenfeld MG, Chen CY, et al. The Wnt/ β -catenin→Pitx2 pathway controls the turnover of Pitx2 and other unstable mRNAs. *Mol Cell*. 2003;12:1201–11.
 37. Luo J, Yao Y, Ji S, Sun Q, Xu Y, Liu K, et al. PITX2 enhances progression of lung adenocarcinoma by transcriptionally regulating WNT3A and activating Wnt/ β -catenin signaling pathway. *Cancer Cell Int*. 2019;19:96.
 38. Amen M, Liu X, Vadlamudi U, Elizondo G, Diamond E, Engelhardt JF, et al. PITX2 and β -catenin interactions regulate Lef-1 isoform expression. *Mol Cell Biol*. 2007;27:7560–73.
 39. Kioussi C, Briata P, Baek SH, Rose DW, Hamblet NS, Herman T, et al. Identification of a Wnt/Dvl/ β -Catenin → Pitx2 pathway mediating cell-type-specific proliferation during development. *Cell*. 2002;111:673–85.
 40. Sun J, Huang X, Niu C, Wang X, Li W, Liu M, et al. aFGF alleviates diabetic endothelial dysfunction by decreasing oxidative stress via Wnt/ β -catenin-mediated upregulation of HXK2. *Redox Biol*. 2021;39:101811.
 41. Guo R, Wang X, Fang Y, Chen X, Chen K, Huang W, et al. rhFGF20 promotes angiogenesis and vascular repair following traumatic brain injury by regulating Wnt/ β -catenin pathway. *Biomed Pharmacother*. 2021;143:112200.

ACKNOWLEDGEMENTS

We express our thanks to Shanghai Bioprofile Technology Co., LTD. for their technical support in RNA-sequencing.

AUTHOR CONTRIBUTIONS

Conceptualization, JX and ZW; Data curation, QG and JL; Formal analysis, QG; Funding acquisition, JX and ZW; Investigation, QG and JL; Methodology, QG and JL; Project administration, ZW; Supervision, JX and ZW; Validation, QG, JL and MY; Visualization, QG; Writing-original draft, QG; Writing-review & editing, JL and JX.

FUNDING

This study was supported by grants from the National Natural Science Foundation of China (Grant NO. 81971377), the Fellowship of China Postdoctoral Science Foundation, Grant/Award Number: 2020M671393 and Jiangsu Province Capability Improvement Project through Science, Technology and Education (NO. ZDXK202219).

COMPETING INTERESTS

The authors declare no competing interests.

ETHICS APPROVAL AND CONSENT TO PARTICIPATE

The Animal Ethics Committee of Nanjing Medical University provided ethical approval (No. IACUC-2307055). All methods were performed in accordance with the relevant guidelines and regulations.

ADDITIONAL INFORMATION

Supplementary information The online version contains supplementary material available at <https://doi.org/10.1038/s41443-024-00965-9>.

Correspondence and requests for materials should be addressed to Jiadong Xia or Zengjun Wang.

Reprints and permission information is available at <http://www.nature.com/reprints>

Publisher's note Springer Nature remains neutral with regard to jurisdictional claims in published maps and institutional affiliations.

Springer Nature or its licensor (e.g. a society or other partner) holds exclusive rights to this article under a publishing agreement with the author(s) or other rightsholder(s); author self-archiving of the accepted manuscript version of this article is solely governed by the terms of such publishing agreement and applicable law.